TRANSIENT HEAT CONDUCTION IN FINITE SLABS WITH

POSITION-DEPENDENT HEAT GENERATION

By Roy W. Miller

Lewis Research Center
Cleveland, Ohio

NATIONAL AERONAUTICS AND SPACE ADMINISTRATION

TRANSIENT HEAT CONDUCTION IN FINITE SLABS WITH

POSITION-DEPENDENT HEAT GENERATION

by Roy W. Miller

Lewis Research Center

SUMMARY

Transient heat conduction in a slab of finite thickness is analyzed so as to include the effect of position-dependent heat generation. One face of the slab is a convecting surface, and the other is considered to be insulated. Temperature distributions are obtained for the cases of constant, linear, exponential, and cosinusoidal heat-production rates. The solutions are obtained by the integral transform method and are in terms of Fourier series. Numerical values of these series were calculated and are presented graphically, in dimensionless form, so that specific cases can be easily computed. The method of solution is outlined in detail so that temperature distributions can be obtained for other position-dependent heat-generation rates.

INTRODUCTION

Heat generation in solids occurs in the fields of electrical, chemical, and nuclear engineering. Closed-form analytical solutions for the resulting conduction temperature distributions are generally limited to simple-shaped bodies with constant heat-production rates.

Transient heat conduction in a slab with one insulated surface and constant heat production is treated in references 1 to 3. Solutions, with numerical results, are given in references 1 and 3 for the case of a slab initially at zero temperature with the uninsulated surface maintained at zero temperature. The solution to the same problem except for a slab with a constant initial temperature is given in reference 2. Also in reference 3, charts are presented for the surface temperature variations when the uninsulated surface is convecting and the slab is initially at the temperature of the surrounding medium.

The conduction problem in the slab initially at zero temperature, with one insulated

and one zero-temperature surface, is developed formally in reference 1 for an arbitrary position-dependent heat-generation rate. The resulting temperature distribution is in the form of an integral, and specific generation functions are not treated.

In the field of nuclear engineering, the heat-generation function is usually not a constant but is a function of position relative to the reactor core (refs. 4 and 5). The detailed form of the generation-rate function depends on factors such as the core configuration. The variation is often cosinusoidal or exponential, and in some cases it can be approximated by a linear variation.

Consideration is given herein to transient heat conduction with position-dependent heat generation in a finite slab that has one insulated and one convecting surface. The slab is initially at a constant temperature. The problem is developed for heat generation with an unspecified variation in the direction of the slab thickness. The cases of constant, linear, exponential, and cosinusoidal heat-production variations are considered in detail.

ANALYSIS

Formulation of Problem

Consider the transient conduction of heat in a homogeneous finite slab with constant properties k, ρ, and c (fig. 1). (Symbols are defined in appendix A.) Initially the slab is at the constant temperature T_i. For $t > 0$, heat is generated in the slab at a rate $G(X)$, which depends on position in the direction normal to the bounding planes. Convection heat transfer occurs at the face $X = 0$ between the body and the surrounding medium, which is at the constant bulk temperature T_b. The convective heat-transfer coefficient is considered constant, and the plane $X = L$ is thermally insulated. Then the governing equation, the initial condition, and the surface conditions are the following (ref. 1):

$$\frac{\partial T}{\partial t} = \alpha \frac{\partial^2 T}{\partial X^2} + \frac{G(X)}{\rho c} \qquad 0 < X < L \tag{1}$$

$$T = T_i \qquad t = 0 \text{ for all } X \tag{2}$$

$$k \frac{\partial T}{\partial X} = h(T - T_b) \qquad \text{at } X = 0, \, t > 0 \tag{3}$$

$$\frac{\partial T}{\partial X} = 0 \qquad \text{at } X = L, \, t > 0 \tag{4}$$

Solutions

The problem defined by equations (1) to (4) can be solved by the method of integral transform. A modified Fourier cosine transform is applied to the space variable. This procedure yields an ordinary differential equation in time and an initial condition for the transformed temperature. Let

$$x = L - X$$

$$\theta = T - T_b$$

Then equations (1) to (4) can be rewritten as follows:

$$\frac{\partial \theta}{\partial t} = \alpha \frac{\partial^2 \theta}{\partial x^2} + \frac{G(x)}{\rho c} \qquad 0 < x < L \tag{1a}$$

$$\theta = T_i - T_b = \theta_i \qquad t = 0 \text{ for all } x \tag{2a}$$

$$\frac{\partial \theta}{\partial x} = -\frac{h}{k} \theta \qquad \text{at } x = L, \ t > 0 \tag{3a}$$

$$\frac{\partial \theta}{\partial x} = 0 \qquad \text{at } x = 0, \ t > 0 \tag{4a}$$

Applying the modified Fourier cosine transform (see appendix B) to equations (1a) and (2a) and noting that $C_1 = C_2 = 0$ give

$$\frac{d\tilde{\theta}}{dt} = -\frac{\alpha \lambda_n^2}{L^2} \tilde{\theta} + \frac{\tilde{G}}{\rho c} \tag{5}$$

$$\tilde{\theta} = \tilde{\theta}_i \qquad t = 0 \tag{6}$$

where

$$\tilde{\theta}_i = \int_0^L \theta_i \cos \frac{\lambda_n x}{L} \, dx = \frac{L \theta_i}{\lambda_n} \sin \lambda_n \tag{7}$$

$$\widetilde{G} = \int_0^L G(x) \cos \frac{\lambda_n x}{L} \, dx \tag{8}$$

and λ_n are the roots of

$$\lambda_n \tan \lambda_n = Bi \tag{B3}$$

The solution to equation (5) with the initial condition (eq. (6)) is

$$\widetilde{\theta} = \widetilde{\theta}_i e^{-\lambda_n^2 Fo} + \left(1 - e^{-\lambda_n^2 Fo} \right) \frac{\widetilde{G} L^2}{k \lambda_n^2} \tag{9}$$

where $Fo = \alpha t / L^2$ is the Fourier number.

Inverting equation (9) gives

$$\theta = \sum_n \frac{2}{(\lambda_n + \sin \lambda_n \cos \lambda_n)} \left[\theta_i e^{-\lambda_n^2 Fo} \sin \lambda_n + \left(1 - e^{-\lambda_n^2 Fo} \right) \frac{\widetilde{G} L}{k \lambda_n} \right] \cos \frac{x}{L} \lambda_n \tag{10}$$

which in terms of the original variables is

$$\frac{T - T_b}{T_i - T_b} = \sum_n \frac{2}{(\lambda_n + \sin \lambda_n \cos \lambda_n)} \left[e^{-\lambda_n^2 Fo} \sin \lambda_n + \left(1 - e^{-\lambda_n^2 Fo} \right) \frac{\widetilde{G} L}{\lambda_n k (T_i - T_b)} \right]$$

$$\times \cos \left[\left(1 - \frac{x}{L} \right) \lambda_n \right] \tag{10a}$$

Thus, for a specific position-dependent heat-generation rate, the transform of the generation function can be evaluated using equation (8). The transient temperature distribution is then given by equation (10a). The cases of constant, linear, exponential, and cosinusoidal heat-generation rates are treated herein.

Constant heat-generation rate. - For a constant heat-generation rate (fig. 2),

$$G(X) = G_0 \qquad t > 0 \tag{11}$$

Then, from equation (8),

$$\widetilde{G} = \int_0^L G_0 \cos \frac{\lambda_n x}{L} \, dx = \frac{G_0 L}{\lambda_n} \sin \lambda_n \tag{12}$$

Substituting equation (12) in equation (10a) gives the following temperature distribution for constant heat production:

$$\frac{T - T_b}{T_i - T_b} = \psi_1 + \frac{G_0 L^2}{k(T_i - T_b)} \psi_2 \tag{13}$$

The position- and time-dependent functions ψ_1 and ψ_2, herein referred to as the transient temperature and uniform temperature functions, respectively, in equation (13) are

$$\psi_1 = \sum_n \frac{2}{(\lambda_n + \sin \lambda_n \cos \lambda_n)} e^{-\lambda_n^2 Fo} \sin \lambda_n \cos\left[\left(1 - \frac{X}{L}\right)\lambda_n\right] \tag{14}$$

$$\psi_2 = \sum_n \frac{2}{(\lambda_n + \sin \lambda_n \cos \lambda_n)} \frac{1 - e^{-\lambda_n^2 Fo}}{\lambda_n^2} \sin \lambda_n \cos\left[\left(1 - \frac{X}{L}\right)\lambda_n\right] \tag{15}$$

where $Fo = \alpha t/L^2$ is the Fourier number and $Bi = hL/k$ is the Biot number. The values of λ_n in equations (14) and (15) are the roots of equation (B3), namely,

$$\lambda_n \tan \lambda_n = Bi \tag{B3}$$

Linearly varying heat-generation rate. - When the heat-generation rate varies linearly (fig. 3), the following equation results:

$$G(X) = G_0 + mX \qquad t > 0 \tag{16}$$

5

where m is the constant (positive or negative) slope of the generation rate. The transformed generation function (eq. (8)) for this case is

$$\tilde{G} = \int_0^L [(G_0 + mL) - mx]\cos\frac{\lambda_n x}{L}\,dx = \frac{G_0 L}{\lambda_n}\sin\lambda_n + \frac{mL^2}{\lambda_n^2}(1 - \cos\lambda_n) \tag{17}$$

and the temperature distribution (eq. (10a)) becomes

$$\frac{T - T_b}{T_i - T_b} = \psi_1 + \frac{G_0 L^2}{k(T_i - T_b)}\psi_2 + \frac{mL^3}{k(T_i - T_b)}\psi_3 \tag{18}$$

The linear temperature function ψ_3 (eq. (18)) is defined as

$$\psi_3 = \sum_n \frac{2}{(\lambda_n + \sin\lambda_n \cos\lambda_n)}\frac{\left(1 - e^{-\lambda_n^2 Fo}\right)(1 - \cos\lambda_n)}{\lambda_n^3}\cos\left[\left(1 - \frac{X}{L}\right)\lambda_n\right] \tag{19}$$

Exponentially varying heat-generation rate. - The heat-generation function for exponential variation (fig. 4) is

$$G(X) = G_0 e^{-\mu(X/L)} \qquad t > 0 \tag{20}$$

where μ is a constant attenuation coefficient (positive or negative). Substituting equation (20) in equation (8) gives

$$\tilde{G} = \int_0^L G_0 e^{-\mu[1-(x/L)]}\cos\frac{\lambda_n x}{L}\,dx = \frac{G_0 L}{\mu^2 + \lambda_n^2}(\mu\cos\lambda_n + \lambda_n\sin\lambda_n - \mu e^{-\mu}) \tag{21}$$

Then, from equation (10a), the temperature distribution is

6

$$\frac{T - T_b}{T_i - T_b} = \psi_1 + \frac{G_0 L^2}{k(T_i - T_b)} \psi_4 \tag{22}$$

where

$$\psi_4 = \sum_n \frac{2}{(\lambda_n + \sin \lambda_n \cos \lambda_n)} \frac{1 - e^{-\lambda_n^2 Fo}}{\lambda_n(\mu^2 + \lambda_n^2)} (\mu \cos \lambda_n + \lambda_n \sin \lambda_n - \mu e^{-\mu}) \cos\left[\left(1 - \frac{X}{L}\right)\lambda_n\right] \tag{23}$$

is the exponential temperature function, and λ_n are the roots of equation (B3).

Cosinusoidally varying heat-generation rate. - The cosinusoidal heat-generation rates indicated in figure 5 are

$$G(X) = G_M \cos \frac{\pi(X + \delta)}{2D} \tag{24}$$

The positive or negative δ in equation (24) is the displacement of the convecting surface from the plane of maximum heat production.

With cosinusoidal heat generation, the transformed generation function is given by

$$\widetilde{G} = \int_0^L G_M \cos \frac{\pi}{2D} [(\delta + L) - x] \cos \frac{\lambda_n x}{L} dx \tag{25}$$

Evaluating the integral gives

$$\widetilde{G} = \frac{G_M L}{d^2 - \lambda_n^2} [d \sin(d + \Delta) - d \sin \Delta \cos \lambda_n - \lambda_n \cos \Delta \sin \lambda_n] \quad \text{when } \lambda_n^2 \neq d^2 \tag{25a}$$

and

$$\widetilde{G} = \frac{G_M L}{2d} [d \cos(d + \Delta) + \cos \Delta \sin d] \quad \text{when } \lambda_n^2 = d^2 \tag{25b}$$

7

where

$$d = \frac{\pi}{2} \frac{L}{D}$$

$$\Delta = \frac{\pi}{2} \frac{\delta}{D}$$

Then the temperature distribution with cosinusoidal heat generation is

$$\frac{T - T_b}{T_i - T_b} = \psi_1 + \frac{G_M L^2}{k(T_i - T_b)} \psi_5 \tag{26}$$

The cosinusoidal temperature function ψ_5 in equation (26) is

$$\psi_5 = \sum_n \frac{2}{(\lambda_n + \sin \lambda_n \cos \lambda_n)} \frac{1 - e^{-\lambda_n^2 Fo}}{\lambda_n \left(d^2 - \lambda_n^2\right)} [d \sin(d + \Delta)$$

$$- d \sin \Delta \cos \lambda_n - \lambda_n \cos \Delta \sin \lambda_n] \cos \left[\left(1 - \frac{X}{L}\right)\lambda_n\right] \quad \text{when } \lambda_n^2 \neq d^2 \tag{27}$$

and

$$\psi_5 = \frac{d \cos(d + \Delta) + \sin d \cos \Delta}{d^2(d + \sin d \cos d)} \left(1 - e^{-d^2 Fo}\right) \cos \left[\left(1 - \frac{X}{L}\right)\lambda_n\right] \quad \text{when } \lambda_n^2 = d^2 \tag{28}$$

RESULTS AND DISCUSSION

Numerical values of the dimensionless time- and position-dependent ψ functions were calculated according to equations (14), (15), (19), (23), and (27). The first six roots of the transcendental equation (eq. (B3)) were used for all calculations. These roots were taken from reference 1. The results are presented graphically in figures 6 to 10.

Individual charts are given for values of dimensionless position X/L from 0 to 1.0

in increments of 0.2. The range of Fourier numbers covered is 0 to 1.4. The Biot numbers included are 0, 0.2, 0.5, 1.0, 2.0, 4.0, 10.0, and ∞. A Biot number of 0 corresponds to an insulated surface. Similarly, the infinite Biot number results apply for the case of a prescribed constant surface temperature T_b.

The transient temperature function ψ_1 is given in figure 6. This function is the dimensionless transient temperature distribution with no heat production that is commonly presented in the literature (e.g., refs. 1 and 6 to 9). The uniform temperature function ψ_2 is given in figure 7. The charts given in reference 3, namely, the temperature-distribution chart for the slab with prescribed surface temperature and the surface-temperature chart for the slab with a convecting surface, are special cases of figure 7. The numerical results are in agreement throughout the range of Fourier number (0 to 0.2) presented in reference 3. The linear temperature function ψ_3 is presented in figure 8. These results apply for positive or negative heat-production-rate slopes. The exponential temperature function ψ_4 depends on the attenuation coefficient μ as well as on X/L, Fo, and Bi. Values of ψ_4 are given in figure 9 for μ values of 0.5, 1.0, 2.0, 4.0, -0.5, -1.0, -2.0, and -4.0. Similar to the preceding case, the cosinusoidal temperature function ψ_5 depends on two additional parameters, d and Δ. Values of ψ_5 for the relative slab thickness d = $\pi/6$ and the displacement of the uninsulated face Δ = -$\pi/3$, -$\pi/6$, 0, and $\pi/6$ are given in figure 10.

For small slab thicknesses, the Fourier number is large even for moderate values of time. Also, for small L, the Biot number will be low except for large values of the convective coefficient. For cases of small thickness, however, the variation of heat generation with position will be small, and uniform production can be assumed. Values of the transient temperature function ψ_1 and the uniform temperature function ψ_2 for large Fourier numbers (0 to 5.0) and small Biot numbers (0 to 4.0) are given in figures 11 and 12, respectively.

The range of the values presented is indicated in the following table for a few specific materials and slab thicknesses:

Material	Slab thickness		Temperature function	Maximum time, min	Minimum convective heat-transfer coefficient, h, for steady state	
	in.	cm			Btu/(hr)(ft^2)($^\circ$R)	J/(hr)(m^2)($^\circ$K)
Stainless steel	4	10.2	All	62	96	1.96×10^6
	2	5.1	Transient	55	48	.98
	2	5.1	Uniform	55	48	.98
Aluminum	12	30.5	All	25	466	9.4 ×10^6
	4	10.2	All	3	1400	28.6
	2	5.1	Transient	2.5	700	14.3
	2	5.1	Uniform	2.5	700	14.3

Figures 6 to 12 should be adequate for most engineering calculations. For values of the parameters not included in these figures, the temperature functions can be computed directly from the series forms presented herein.

As an example of the effect of heat-generation position dependence on the conduction temperature distributions, consider the case of an aluminum rod 1 foot (0.305 m) long under the following conditions:

$$h = 240 \text{ Btu/(hr)(ft}^2\text{)(}^{\circ}\text{R)}; \quad 4.9\times10^6 \text{ J/(hr)(m}^2\text{)(}^{\circ}\text{K)}$$

$$T_b = 200^{\circ} \text{ R}; \quad 111^{\circ} \text{ K}$$

$$T_i = 200^{\circ} \text{ R}; \quad 111^{\circ}\text{K}$$

$$G_0 = 200\,000 \text{ Btu/(hr)(ft}^3\text{)}; \quad 74.6\times10^8 \text{ J/(hr)(m}^3\text{)}$$

$$k = 120 \text{ Btu/(hr)(ft)(}^{\circ}\text{R)}; \quad 0.746\times10^6 \text{ J/(hr)(m)(}^{\circ}\text{K)}$$

$$\alpha = 3.33 \text{ ft}^2\text{/hr}; \quad 0.310 \text{ m}^2\text{/hr}$$

Then, $B_i = hL/k = 2.0$ and $Fo = \alpha t/L^2 = 0.0555\,t$, where t is in minutes.

The case of exponential heat generation with $\mu = 1.0$ is compared with the case of uniform heat generation with a constant value of G_0. From equations (22) and (13),

$$T = T_b + \frac{G_0 L^2}{k} \psi_4 = 200 + 1670 \psi_4 \; (^{\circ}\text{R}); \quad 111 + 927 \psi_4 \; (^{\circ}\text{K}) \text{ for the exponential case}$$

$$T = T_b + \frac{G_0 L^2}{k} \psi_2 = 200 + 1670 \psi_2 \; (^{\circ}\text{R}); \quad 111 + 927 \psi_2 \; (^{\circ}\text{K}) \text{ for the uniform case}$$

The values of ψ_4 and ψ_2 are obtained from figures 9 and 7, respectively.

The time-temperature history at the insulated end of the rod is shown in figure 13. The calculated temperatures are considerably higher under the condition of uniform generation. Also, the time predicted to reach a specified temperature (say 860° R or 478° K) is much less for the uniform-generation case.

10

The temperature distributions at $t = 15$ minutes are shown in figure 14. At all positions in the rod, the predicted temperature values with uniform generation are higher than values calculated for exponential heat production. Figure 14 also shows that temperature gradients under the condition of uniform generation are larger than with exponential heat generation.

CONCLUDING REMARKS

The transient conduction of heat in a solid bounded by two parallel planes was analyzed so as to include the effect of position-dependent heat production. It was assumed that the solid is homoegeneous with constant physical properties and constant initial temperature. The slab with one convecting surface and one insulated surface was considered. Heat-production rates varying constantly, linearly, exponentially, and cosinusoidally in the direction normal to the bounding planes were treated in detail.

The solutions in terms of Fourier series were obtained by the integral transform method. The temperature distributions depend on position, time (Fourier number), convection coefficient (Biot number), and parameters that reflect the specific form of the heat-generation rate. Numerical values of the temperature-distribution series were calculated and are presented graphically in dimensionless form. The range of variables was so selected that specific cases can be easily computed.

The solution procedure is presented for a heat-generation rate with an unspecified variation in the direction of the slab thickness. Thus, by following the outlined procedure, transient temperature distributions can be determined for specific position-dependent heat-generation rates other than those treated in detail in this report.

Lewis Research Center,
    National Aeronautics and Space Administration,
        Cleveland, Ohio, April 20, 1967.

APPENDIX A

SYMBOLS

Bi   Biot number, hL/k

C_1, C_2 constants

c   specific heat

D   quarter wavelength for cosine generation

d   dimensionless slab thickness, $(\pi/2)(L/D)$

e   exponential base

Fo   Fourier number, $\alpha t/L^2$

$\tilde{f}$ modified Fourier cosine transform defined by eq. (B1)

G   volumetric heat-generation rate

h   convective heat-transfer coefficient

k   thermal conductivity

L   slab thickness

m   slope of linearly varying heat-generation rate

T   temperature

T_b bulk temperature of surroundings

t   time

X   coordinate in direction of slab thickness

x   coordinate $L-X$

α thermal diffusivity, $k/\rho c$

Δ dimensionless displacement, $(\pi/2)(\delta/D)$

δ displacement of convecting face for cosinusoidal heat generation

θ temperature difference, $T - T_b$

λ_n roots of eq. (B3)

μ attentuation coefficient for exponential heat-generation rate

ρ density

ψ_1 transient temperature function defined by eq. (14)

ψ_2 uniform temperature function defined by eq. (15)

ψ_3 linear temperature function defined by eq. (19)

ψ_4 exponential temperature function defined by eq. (23)

ψ_5 cosinusoidal temperature function defined by eqs. (27) and (28)

Subscripts:

i   initial

M   maximum

n   1, 2, 3, . . .

0   value at $X = 0$

APPENDIX B

MODIFIED FOURIER COSINE TRANSFORM

The modified Fourier cosine transform used to solve the system of equations (1a) to (4a) is defined (refs. 10 and 11) as

$$\tilde{f}(n) = \int_0^L f(x) \cos \frac{\lambda_n x}{L} \, dx \tag{B1}$$

where the function $f(x)$ must satisfy the Dirichlet conditions (i. e., bounded with a finite number of maxima and minima and a finite number of points of discontinuity). The boundary conditions of the problem are

$$\left. \begin{aligned} \frac{df}{dx} &= C_1 && \text{at } x = 0 \\[2ex] \frac{df}{dx} &= -\frac{h}{k} f + C_2 && \text{at } x = L \end{aligned} \right\} \tag{B2}$$

In equation (B1) λ_n are the roots of

$$\lambda_n \tan \lambda_n = \frac{hL}{k} = Bi \tag{B3}$$

The transform of the Laplacian of f turns out to be

$$\frac{\widetilde{d^2 f}}{dx^2} = -\frac{\lambda_n^2}{L^2} \tilde{f} - C_1 + C_2 \cos \lambda_n \tag{B4}$$

The inversion formula is

$$f(x) = \sum_n \tilde{f}(n) \frac{2\left(\lambda_n^2 + Bi^2\right)}{L\left[\left(\lambda_n^2 + Bi^2\right) + Bi\right]} \cos \frac{x}{L} \lambda_n \tag{B5}$$

13

REFERENCES

1. Carslaw, H. S.; Jaeger, J. C.: Conduction of Heat in Solids. Second ed., Clarendon Press (Oxford), 1959.

2. Schneider, Paul J.: Conduction Heat Transfer. Addison-Wesley Pub. Co., 1955.

3. Heisler, M. P.: Temperature Charts for Internal Heat Generation. ASME Trans., vol. 78, Aug. 1956, pp. 1187-1192.

4. Dietrick, J. R.; and Okrent, D.: Spatial Distribution of Heat Generation. Engineering. Vol. 2 of The Reactor Handbook. J. F. Hogerton and R. C. Grass, eds. AEC Rep. No. AECD-3646, vol. 2, May 1955, pp. 87-121.

5. Glasstone, Samuel; and Sesonske, Alexander: Nuclear Reactor Engineering. D. Van Nostrand, Inc., 1963.

6. Kreith, Frank: Principles of Heat Transfer. International Textbook Co., 1958.

7. Eckert, E. R. G.; and Drake, Robert M., Jr.: Heat and Mass Transfer. Second ed., McGraw-Hill Book Co., Inc., 1959.

8. McAdams, William H.: Heat Transmission. Third ed., McGraw-Hill Book Co., Inc., 1954.

9. Jakob, Max: Heat Transfer. Vol. I, John Wiley and Sons, Inc., 1949.

10. Sneddon, Ian N.: Fourier Transforms. McGraw-Hill Book Co., Inc., 1951.

11. Kaplan, S.; and Sonnemann, G.: A Generalization of the Finite Integral Transform Technique and Tables of Special Cases. Proceedings of the 4th Midwestern Conference on Solid Mechanics, 1959, pp. 497-513.
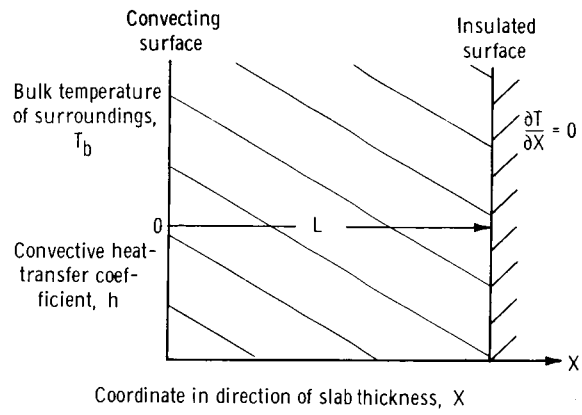
Figure 1. - Finite slab.
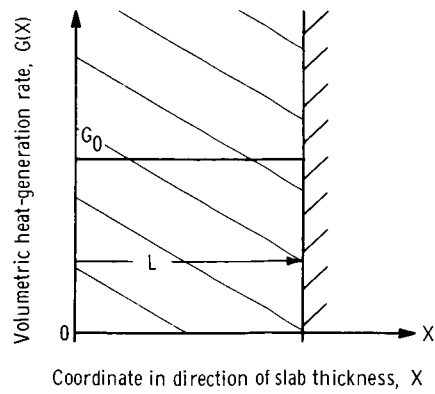
Figure 2. - Slab with constant heat-
generation rate.
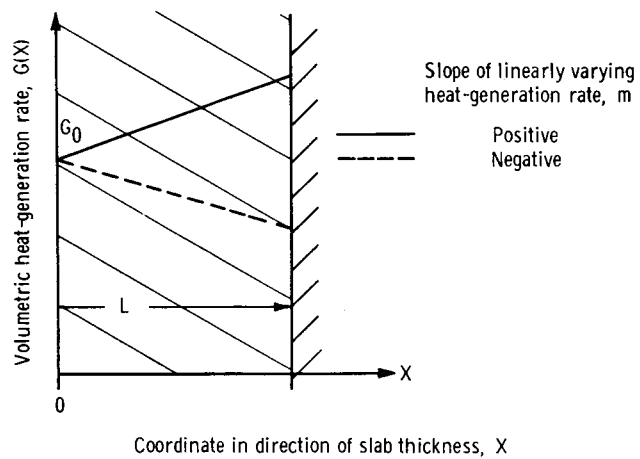
Figure 3. - Slab with linearly varying heat-generation rate.
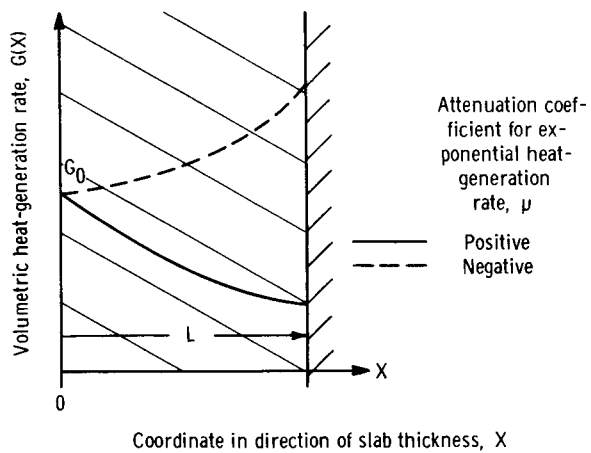
Figure 4. - Slab with exponentially varying heat-generation rate.
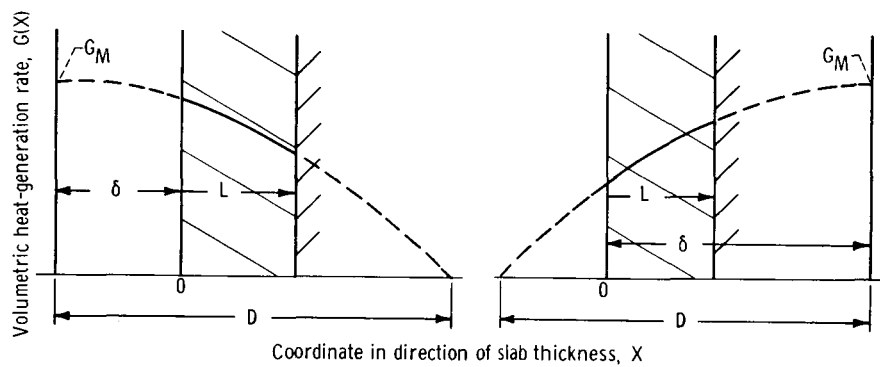
(a) Positive displacement of convecting face.   (b) Negative displacement of convecting face.

Figure 5. - Cosinusoidally varying heat-generation rates where D is quarter wavelength for cosine generation, G_M is maximum volumetric heat-generation rate, L is slab thickness, and δ is displacement of convecting face for cosinusoidal heat generation.
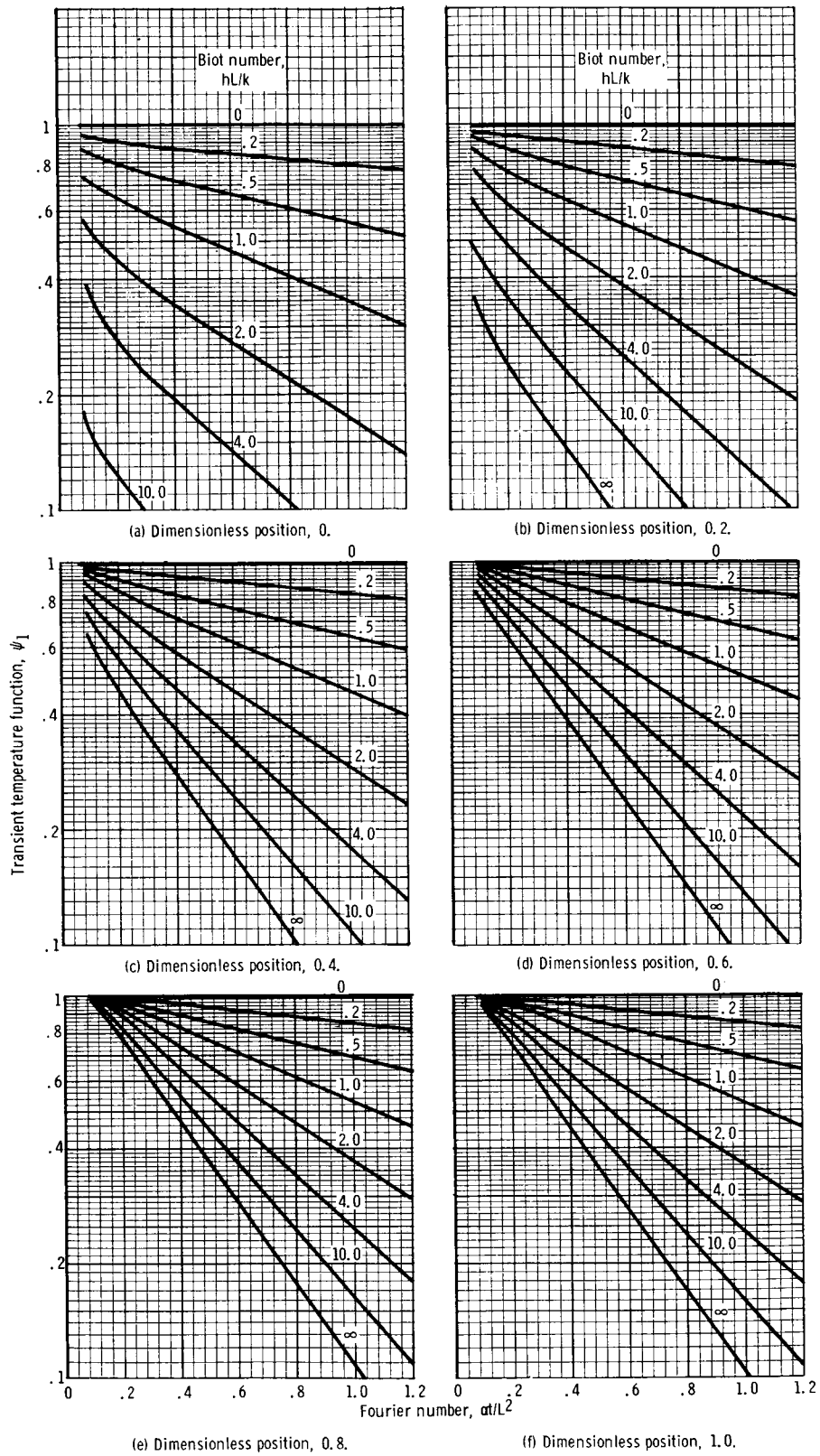
Figure 6. – Response of transient temperature function ψ_1 for slab subjected to sudden change in environmental temperature.
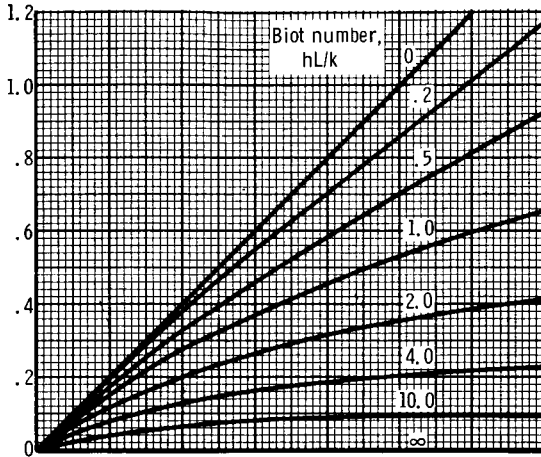
(a) Dimensionless position, 0.
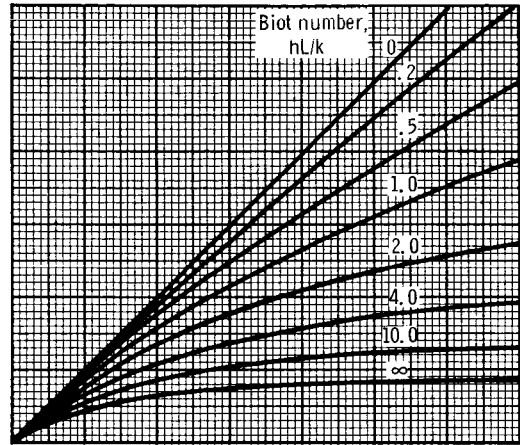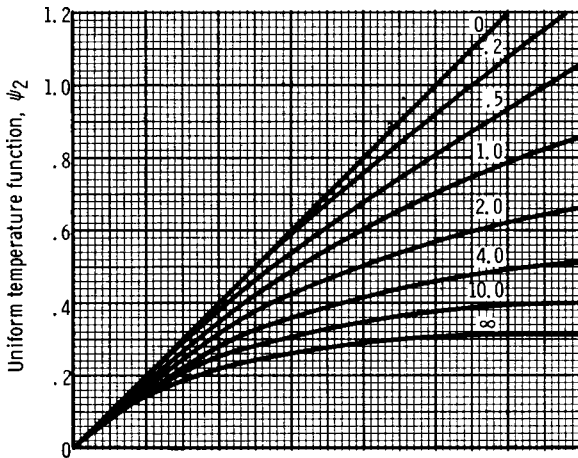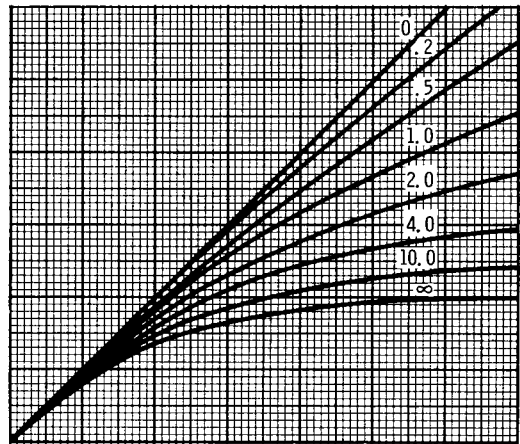
(b) Dimensionless position, 0.2.

(c) Dimensionless position, 0.4.

(d) Dimensionless position, 0.6.
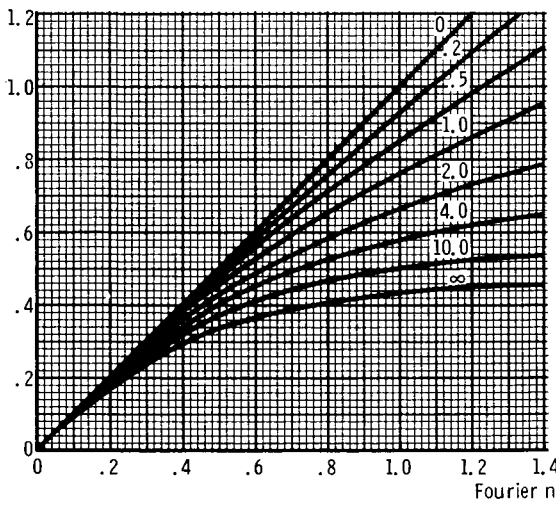
(e) Dimensionless position, 0.8.
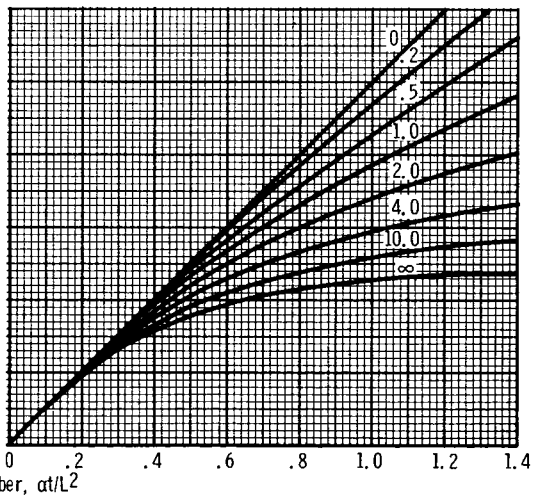
(f) Dimensionless position, 1.0.

Figure 7. - Response of uniform temperature function ψ_2 for slab with uniform internal heat generation.

19

(a) Dimensionless position, 0.

(b) Dimensionless position, 0.2.

(c) Dimensionless position, 0.4.

(d) Dimensionless position, 0.6.

(e) Dimensionless position, 0.8.

(f) Dimensionless position, 1.0.
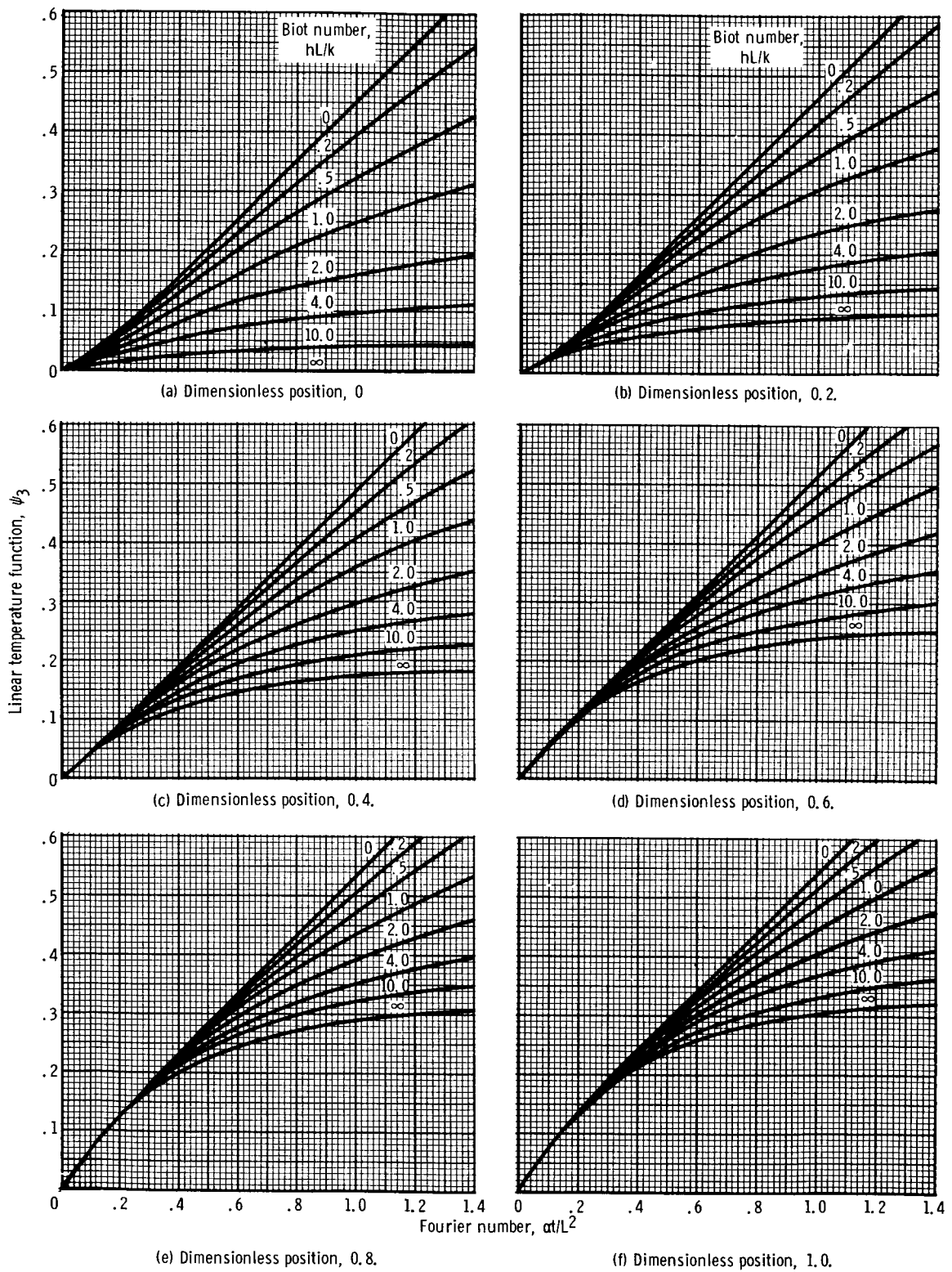
Figure 8. – Response of linear temperature function ψ_3 for slab with heat generation varying linearly in direction of slab thickness.
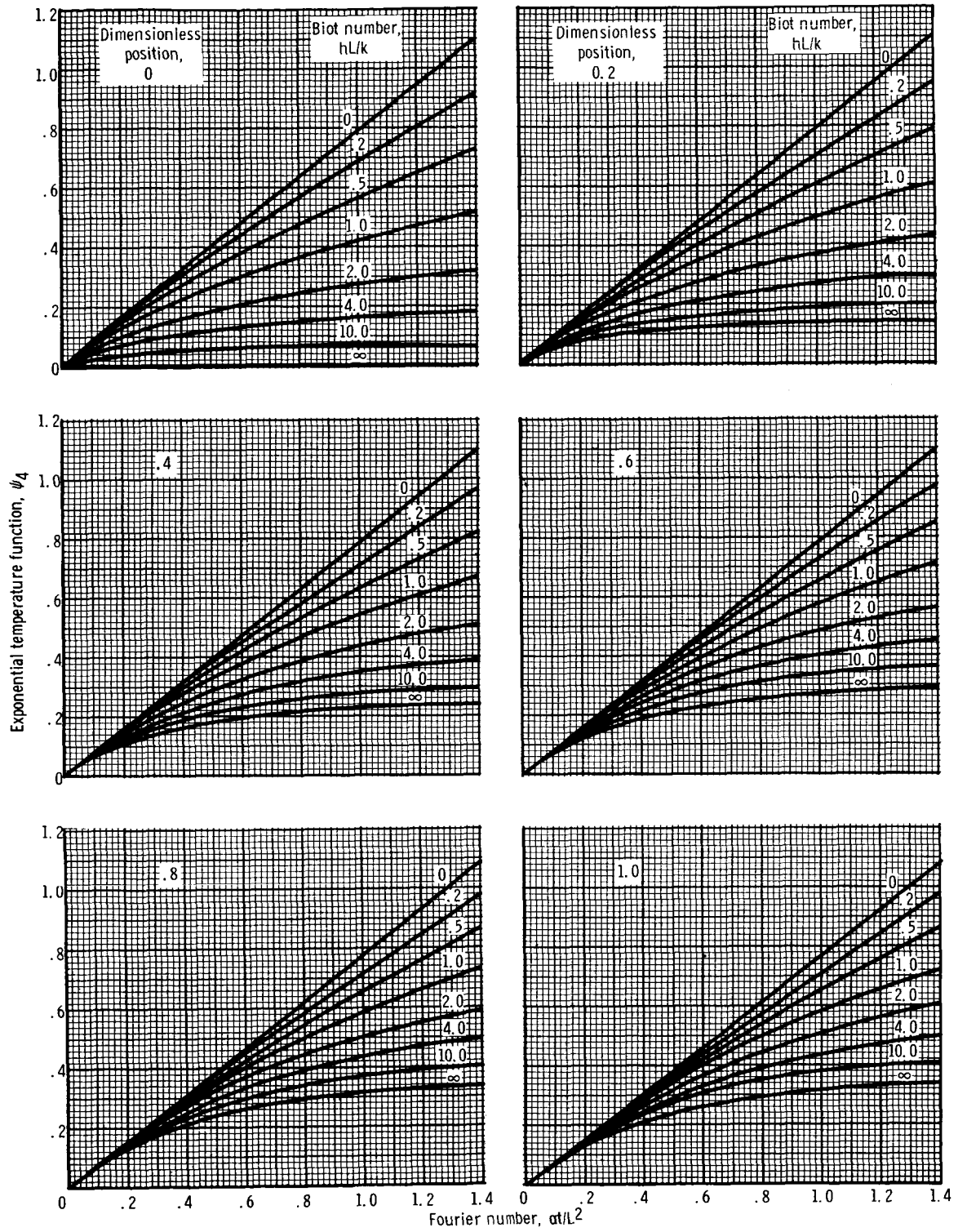
(a) Attenuation coefficient, 0.5.

Figure 9. - Response of exponential temperature function ψ_4 for slab with heat generation varying exponentially in direction of slab thickness.
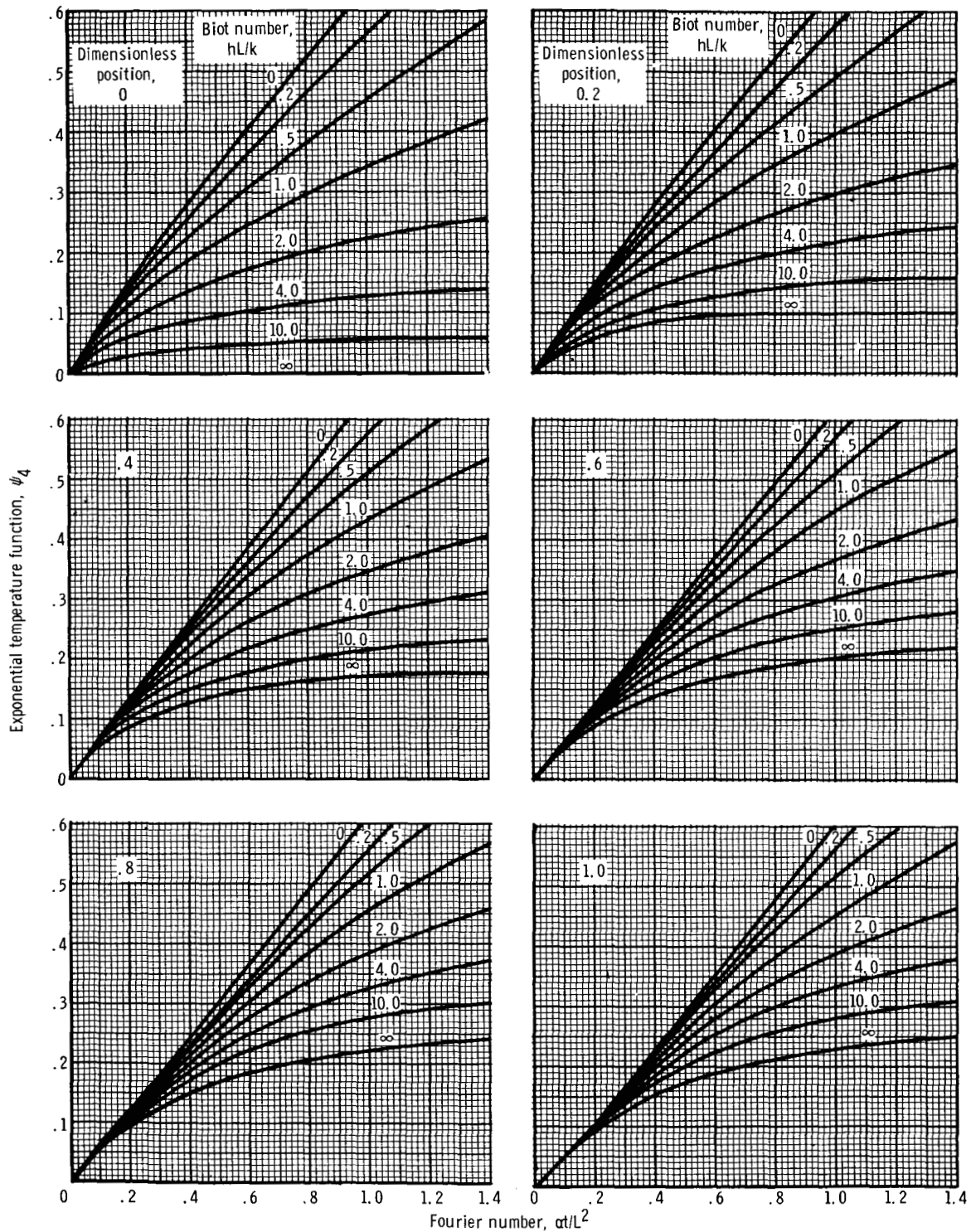
(b) Attenuation coefficient, 1.0.
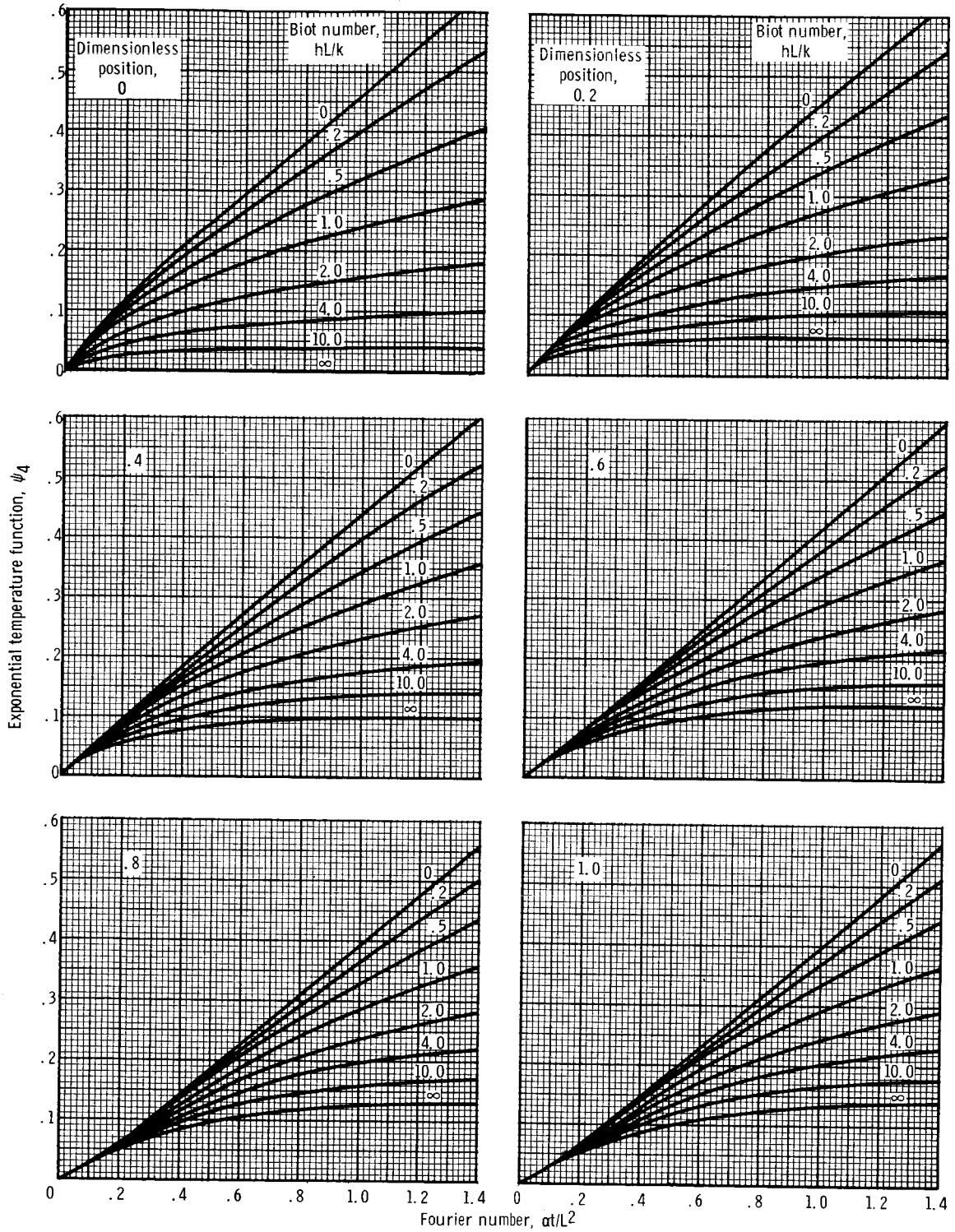
Figure 9. - Continued.

(c) Attenuation coefficient, 2.0.
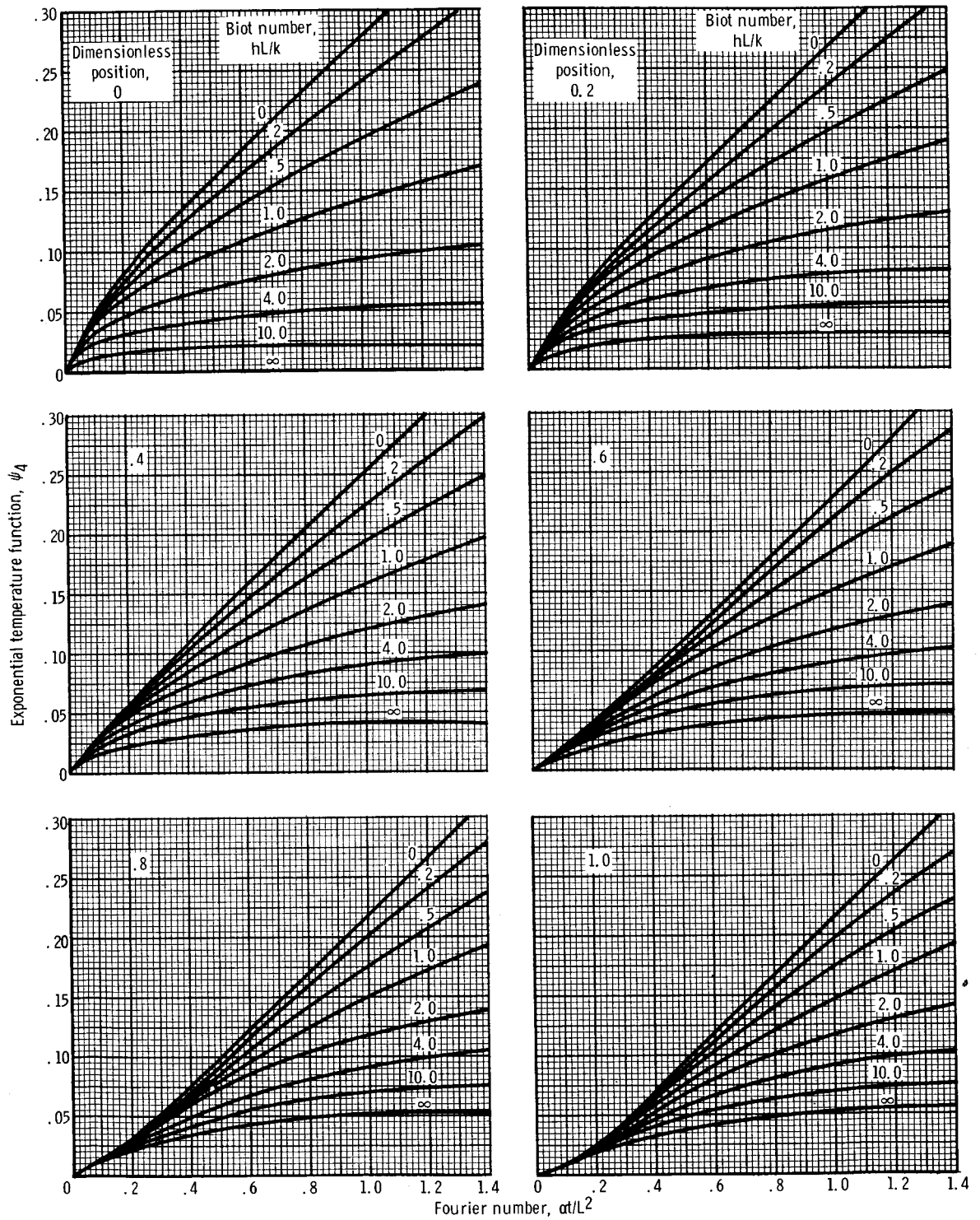
Figure 9. - Continued.

(d) Attenuation coefficient, 4.0.

Figure 9. - Continued.
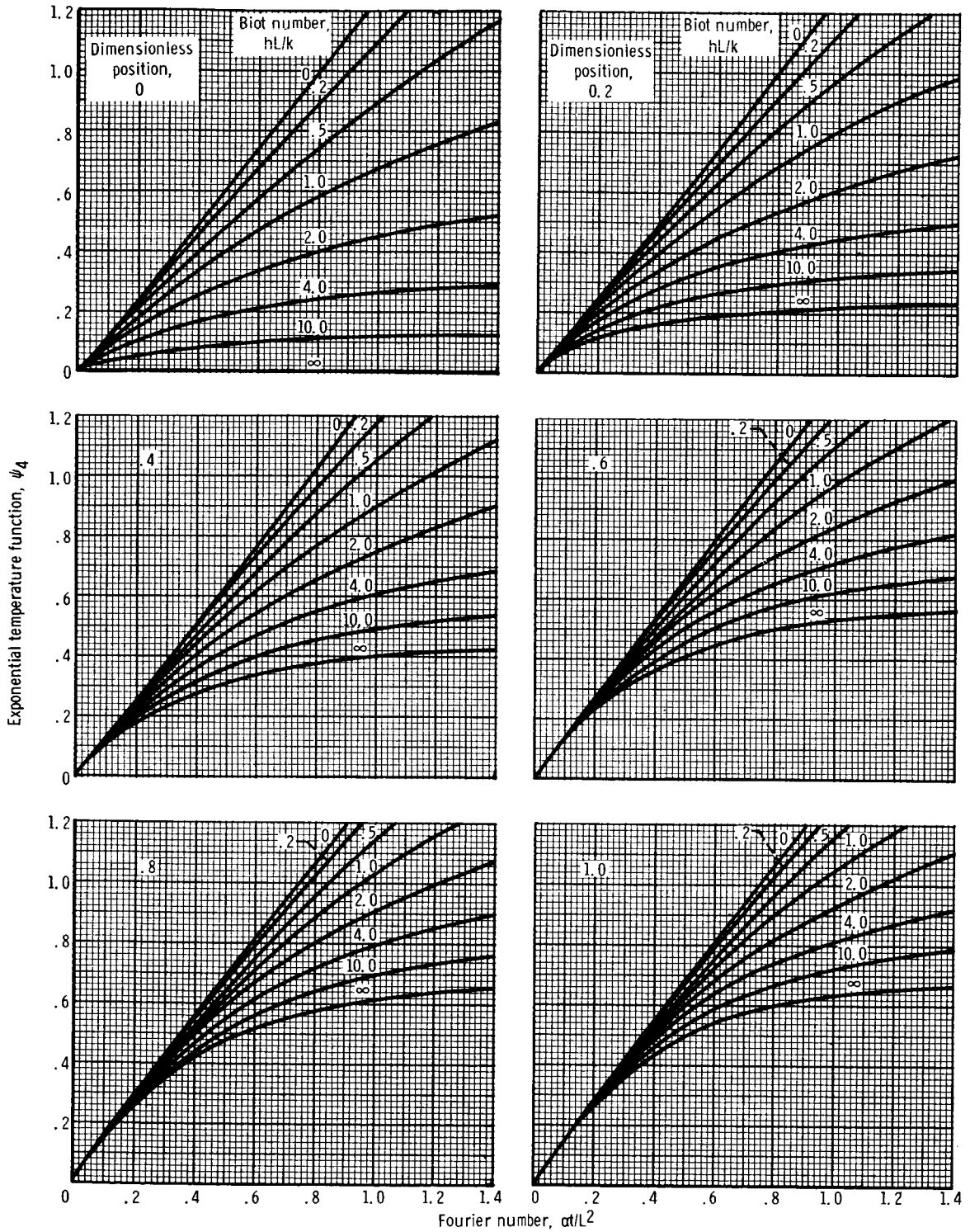
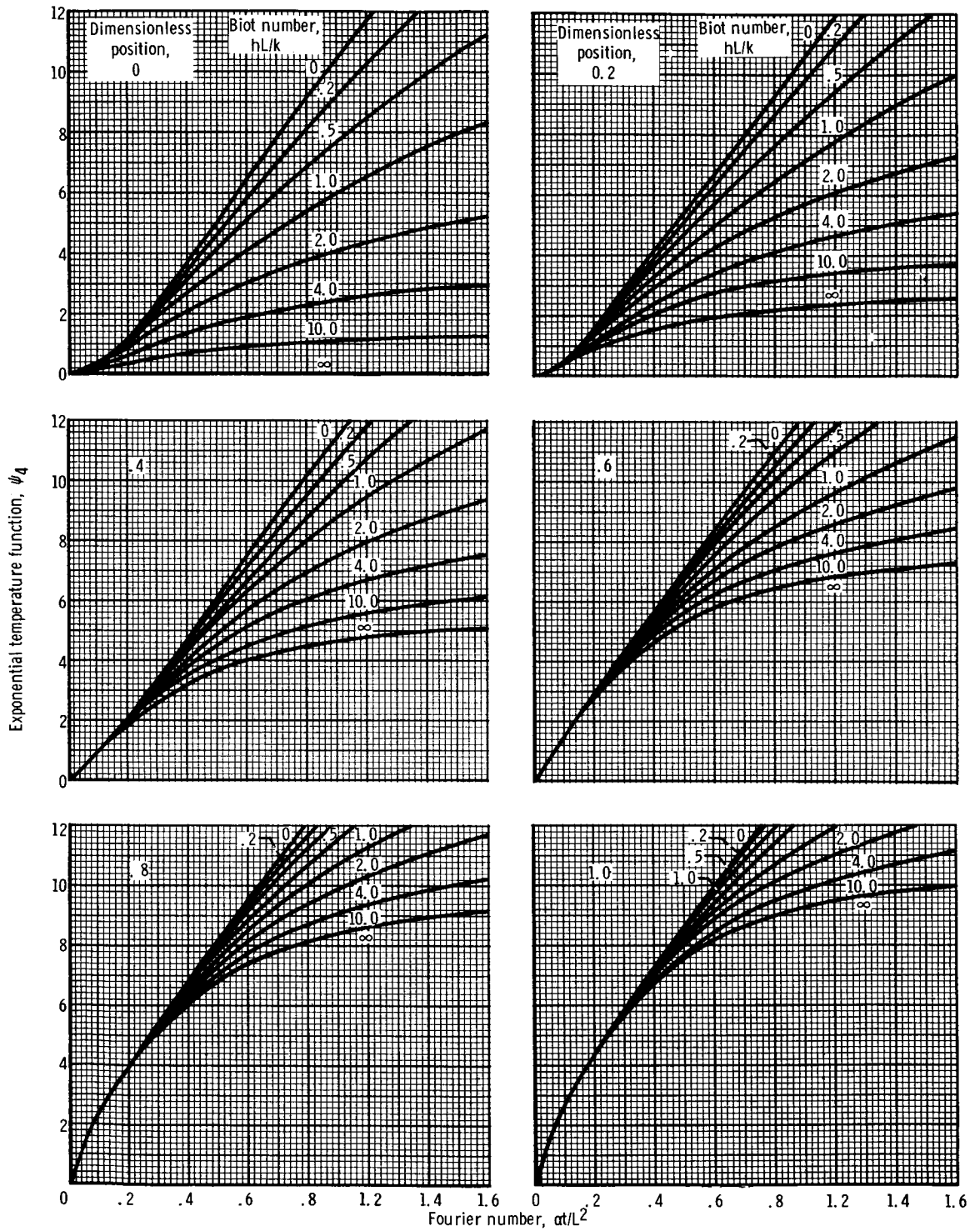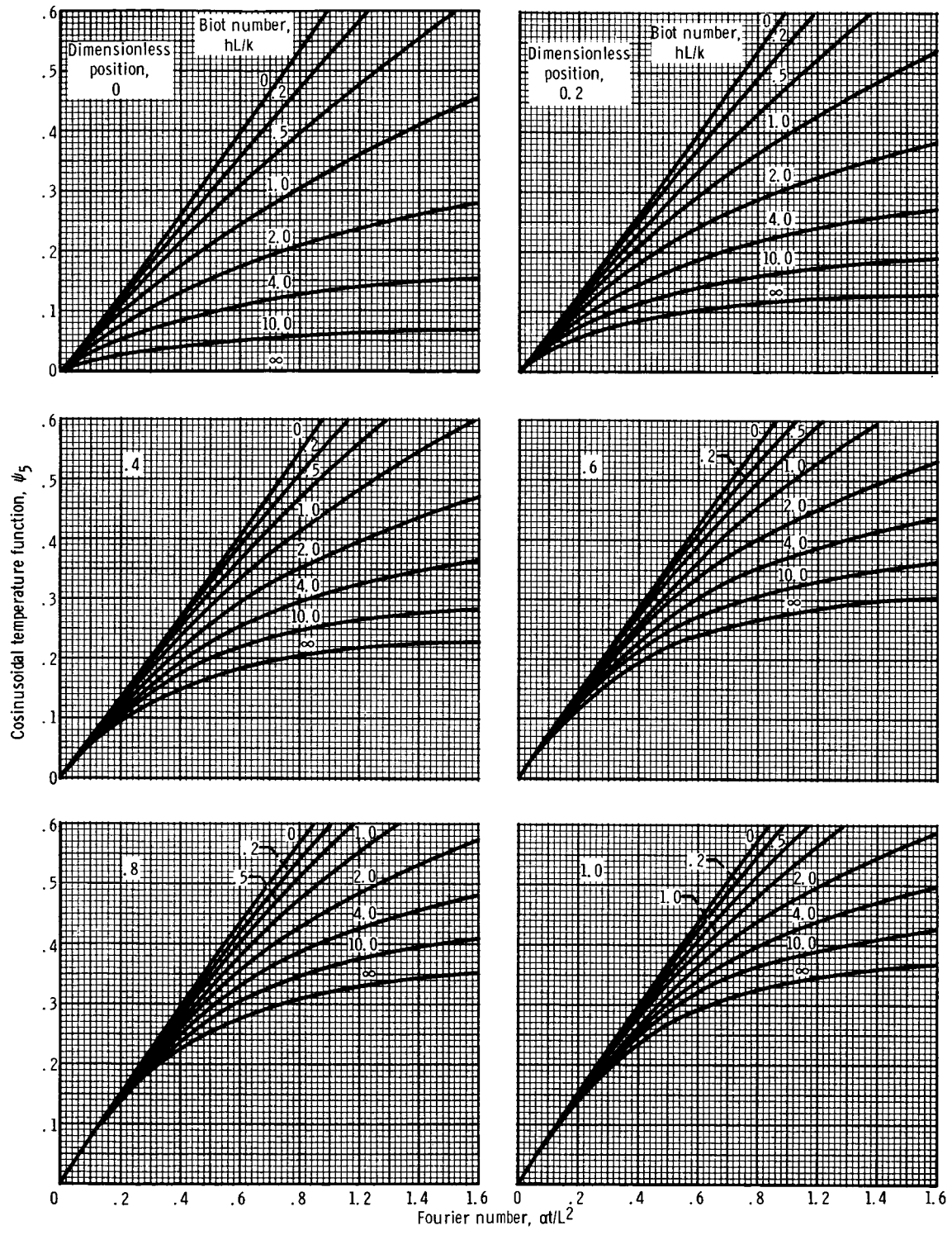(e) Attenuation coefficient, -0.5.

Figure 9. - Continued.
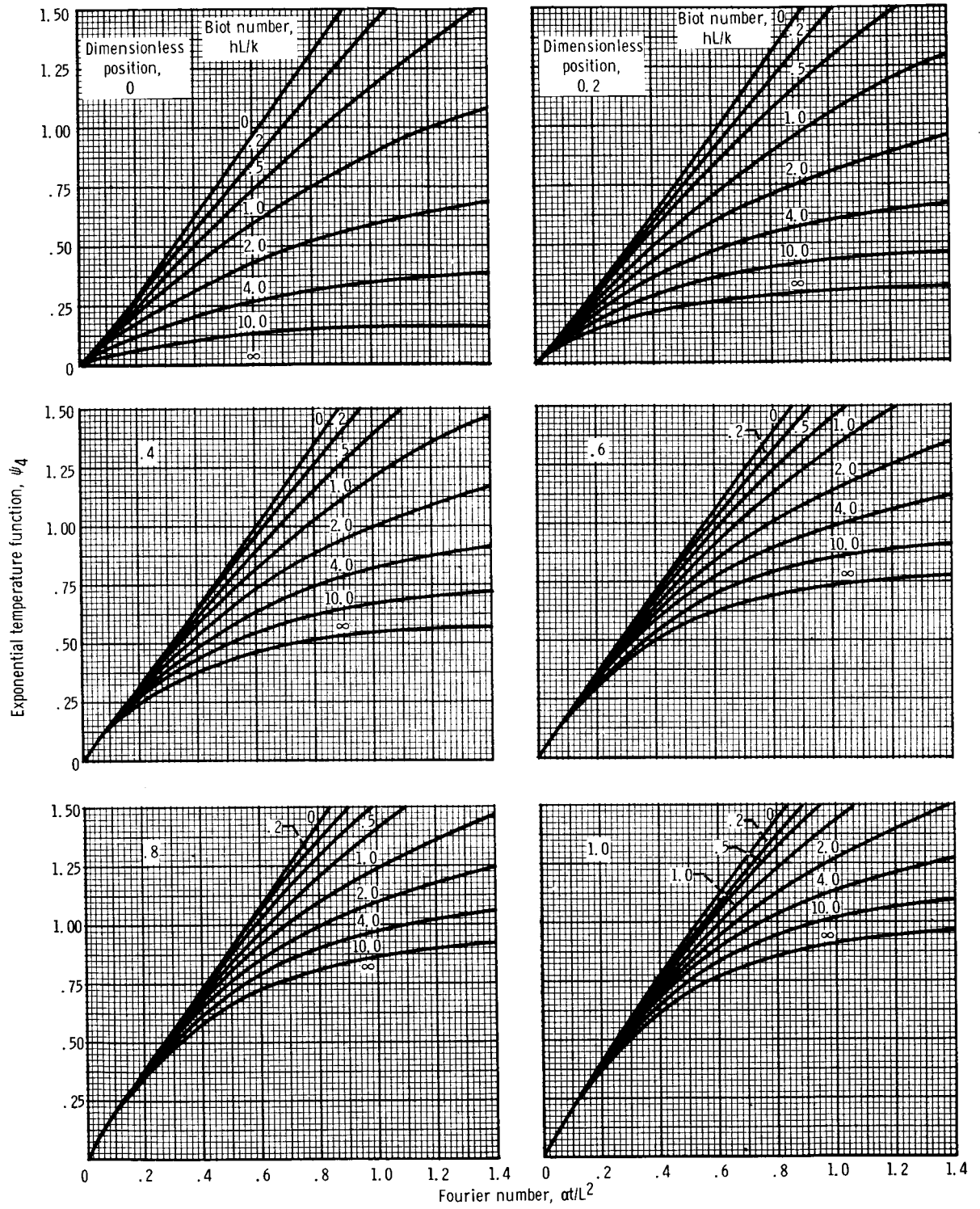
(f) Attenuation coefficient, -1.0.
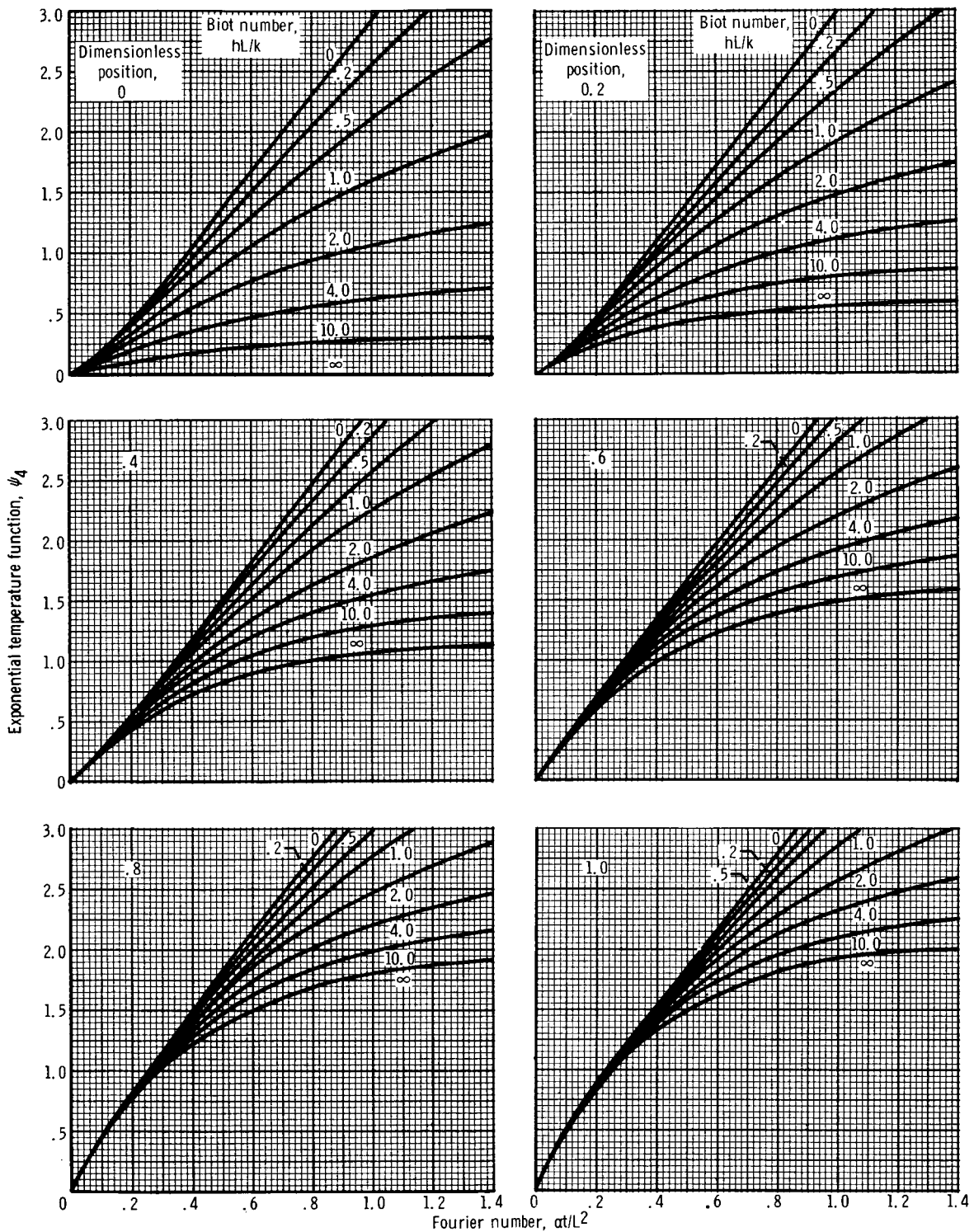
Figure 9. - Continued.

(g) Attenuation coefficient, -2.0.

Figure 9. – Continued.

(h) Attenuation coefficient, -4.0.
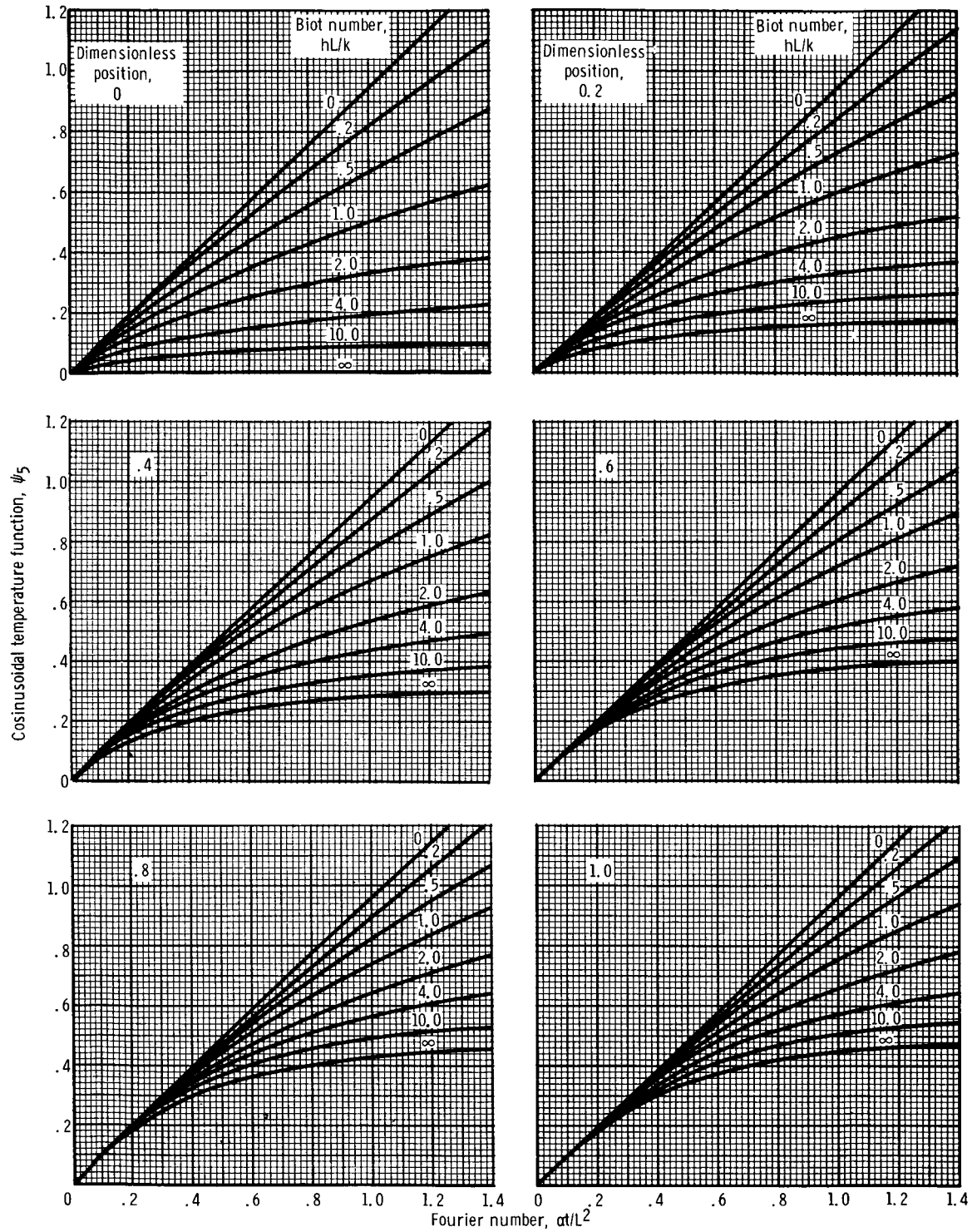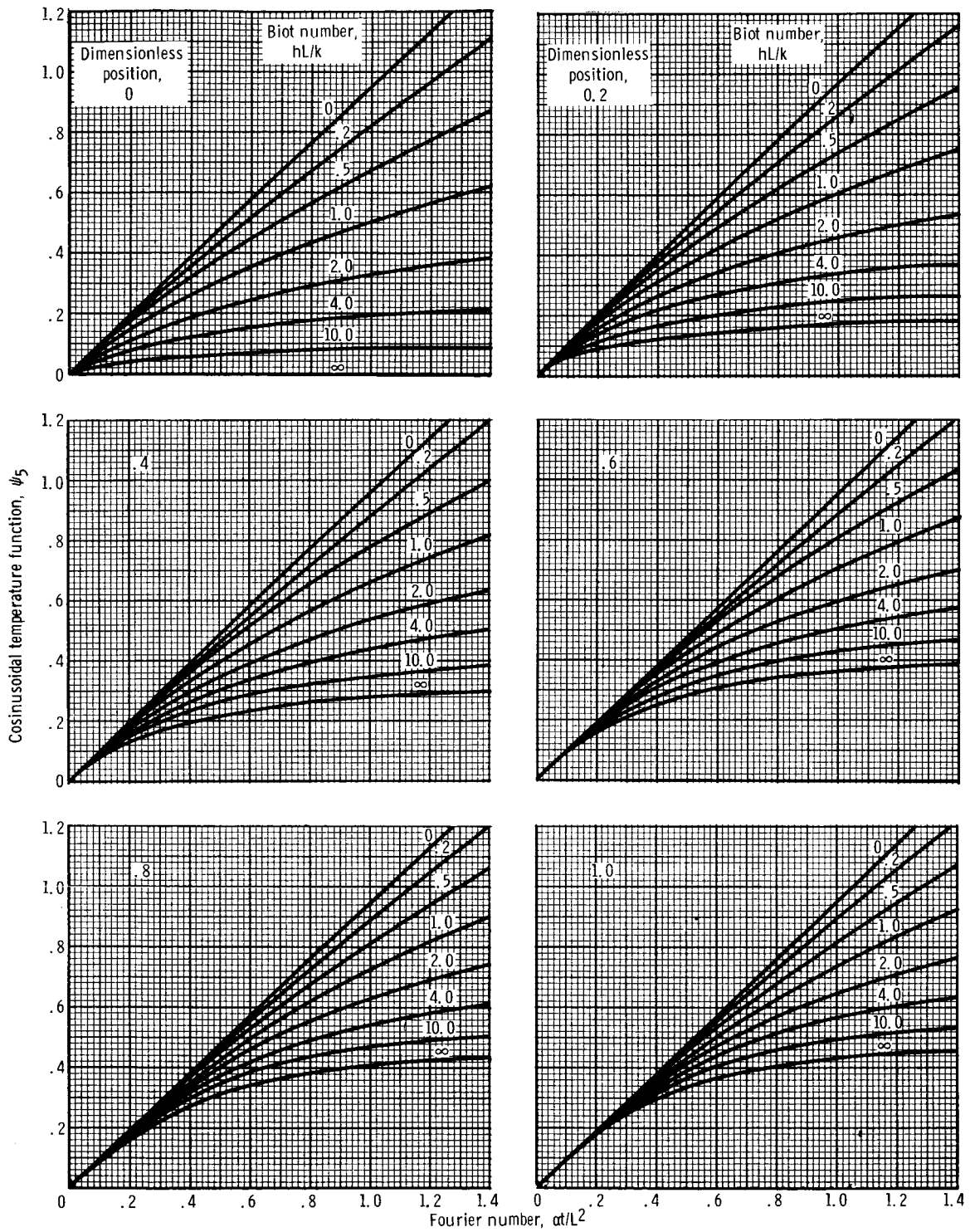
Figure 9. - Concluded.

(a) Dimensionless slab thickness, $\pi/6$; dimensionless displacement, $-\pi/3$.

Figure 10. – Response of cosinusoidal temperature function ψ_5 for slab with heat generation varying cosinusoidally in direction of slab thickness.
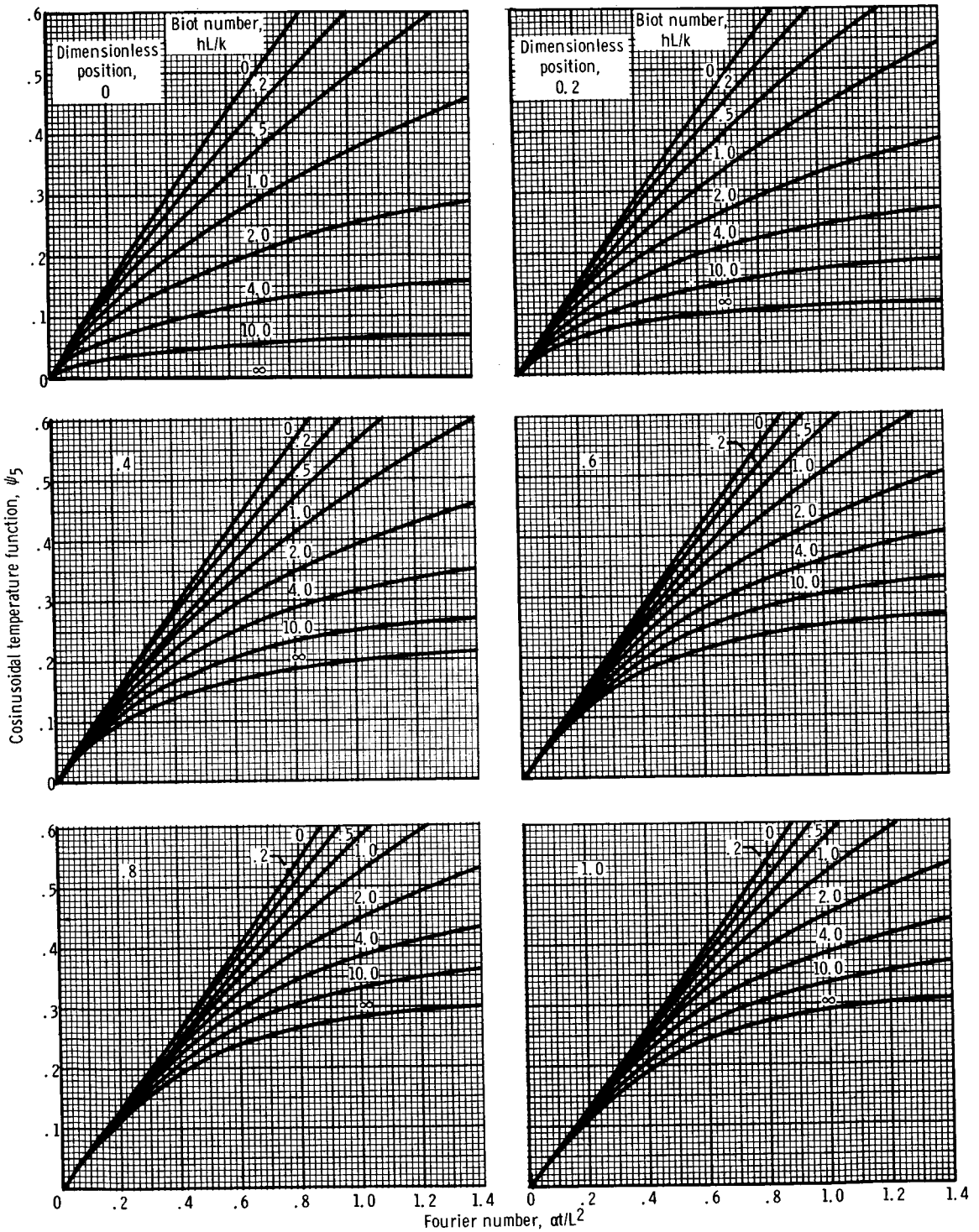
(b) Dimensionless slab thickness, $\pi/6$; dimensionless displacement, $-\pi/6$.

Figure 10. - Continued.

(c) Dimensionless slab thickness, $\pi/6$, dimensionless displacement, 0.

Figure 10. - Continued.

(d) Dimensionless slab thickness, $\pi/6$; dimensionless displacement, $\pi/6$.
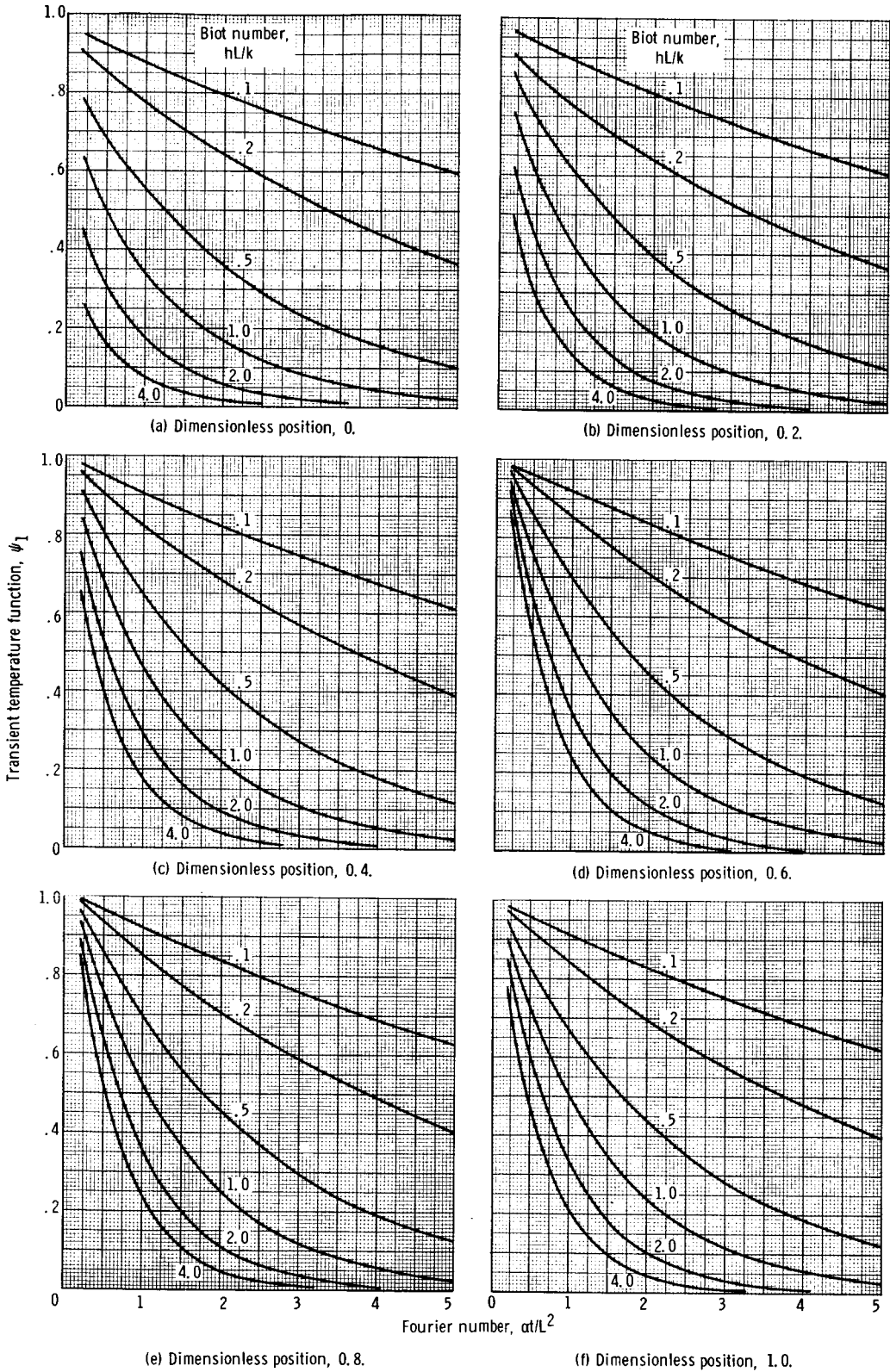
Figure 10. – Concluded.

(a) Dimensionless position, 0.

(b) Dimensionless position, 0.2.

(c) Dimensionless position, 0.4.

(d) Dimensionless position, 0.6.

(e) Dimensionless position, 0.8.

(f) Dimensionless position, 1.0.

Figure 11. – Response of transient temperature function ψ_1 for slab subjected to sudden change in environmental temperature; high Fourier number and low Biot number.

(a) Dimensionless position, 0.

(b) Dimensionless position, 0.2.

(c) Dimensionless position, 0.4.

(d) Dimensionless position, 0.6.

(e) Dimensionless position, 0.8.
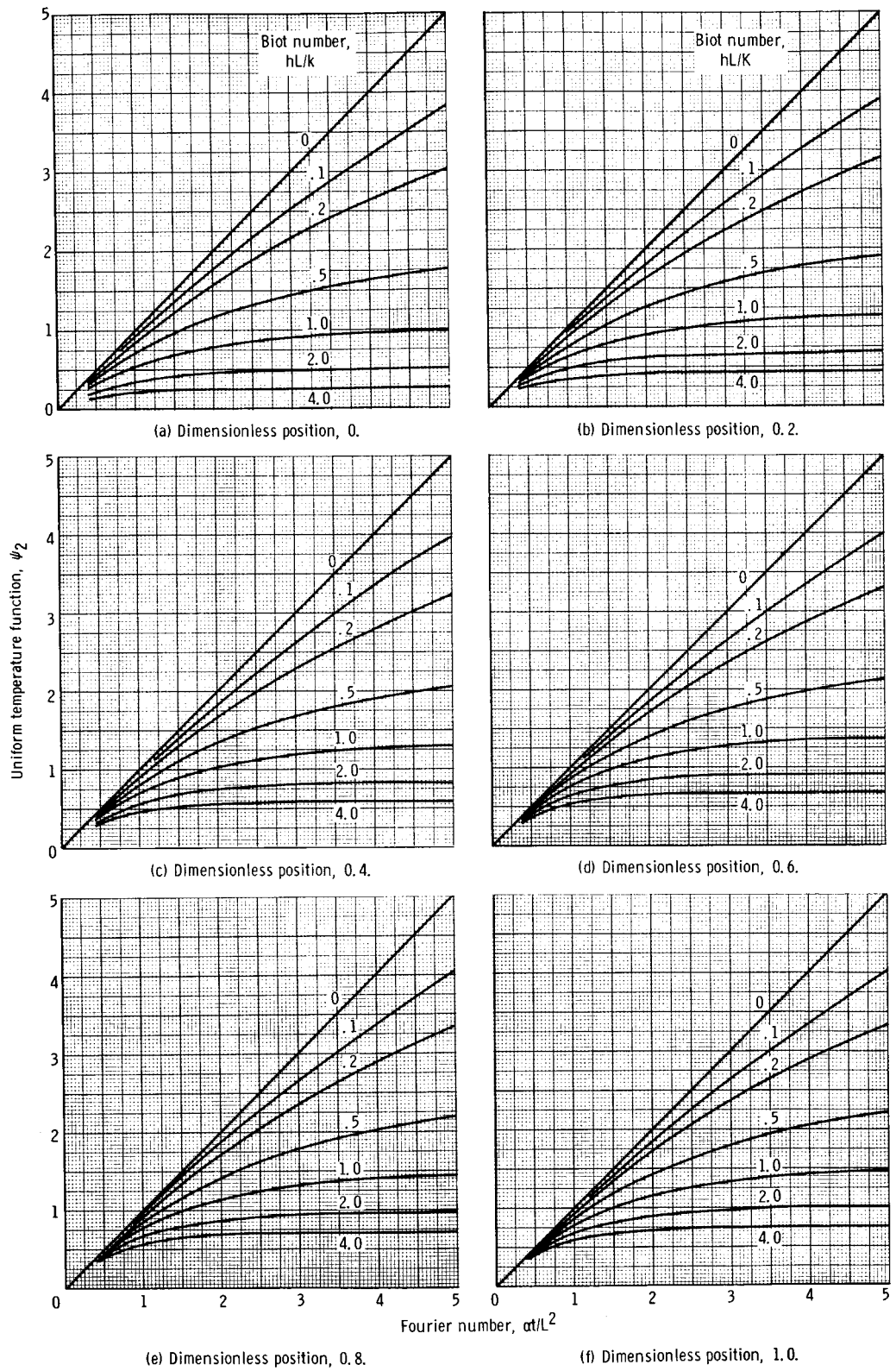
(f) Dimensionless position, 1.0.

Figure 12. - Response of uniform temperature function ψ_2 for slab with uniform internal heat generation; high Fourier number and low Biot number.
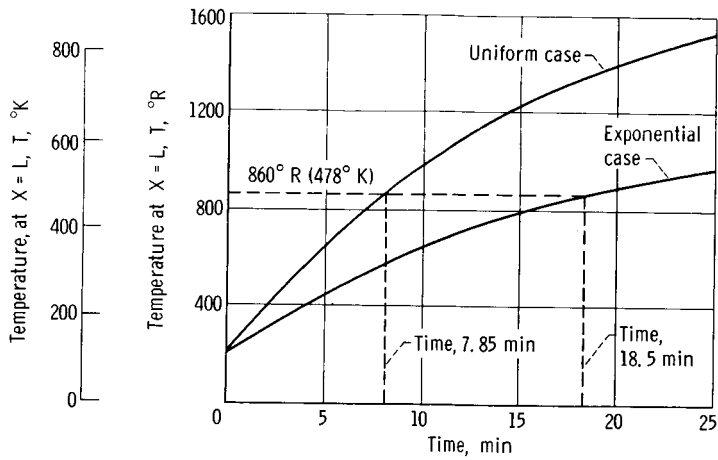
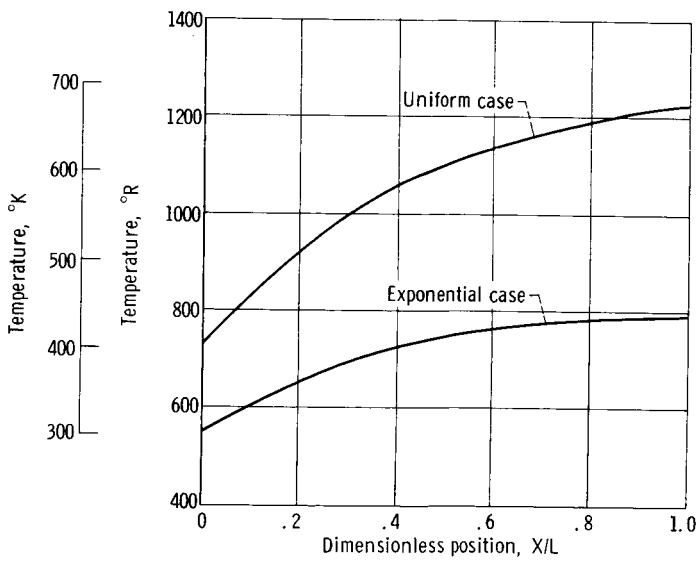Figure 13. - Time-temperature history at insulated end of sample rod.

Figure 14. - Temperature distributions after 15 minutes of heating time for sample rod.